Synthesis and Characterization of PMMA/Organomodified Montmorillonite Nanocomposites Prepared by in Situ Bulk Polymerization

Alexandros K. Nikolaidis, Dimitris S. Achilias,* and George P. Karayannidis

Laboratory of Organic Chemical Technology, Department of Chemistry, Aristotle University of Thessaloniki, Thessaloniki, 541 24 Greece

The effect of the amount of nanofiller and type of organic modifier in organomodified montmorillonite (OMMT)/poly(methyl methacrylate) (PMMA) nanocomposites prepared by in situ bulk polymerization was investigated. Several commercial OMMTs under the tradename Cloisite were used. The structure and morphology of the prepared materials were investigated by means of wide angle X-ray diffraction (WAXD), scanning electron microscopy (SEM), and transmission electron microscopy (TEM) analysis. It was found that the presence of OMMT enhances polymerization kinetics especially in the gel-effect region, while sodium MMT acts rather as a reaction retarder. The presence of the nanofiller increased the thermal stability of the nanocomposites, as measured by thermogravimetric analysis (TGA) and their glass transition temperature, measured by differential scanning calorimetry (DSC), as well as their average molecular weight measured by gel permeation chromatography (GPC). Tensile measurements using a dynamometer revealed an increase in the Young's modulus with the amount of the nanofiller accompanied by a decrease in the tensile strength and elongation at break. Overall, the best performance was found for the nanocomposites of PMMA with Cloisite 25A.

Introduction

Polymers reinforced with a small amount of montmorillonite (MMT) clay have attracted a great deal of research interest in the past decade. These nanocomposites exhibit improved mechanical properties, enhanced thermal stability, fire retardancy, better gas barrier properties, and corrosion resistance.[1] Excellent reviews on polymer-layered silicate nanocomposites have been recently published.[2−4] From the structural point of view, two idealized polymer−clay nanocomposites are possible: intercalated and exfoliated.[4] Intercalation results from the penetration of polymer chains into the clay's interlayer region and interlayer expansion. Usually, the ordered layer structure is preserved and can be detected by X-ray diffraction (XRD). By contrast, exfoliation involves extensive polymer penetration and silicate crystallites delamination, and the individual nanometer-thick silicate platelets are randomly dispersed in the polymer matrix. Exfoliated nanocomposites usually provide the best property enhancement, due to the large aspect ratio and surface area of the clay.[5] Moreover, since clay is naturally hydrophilic and inherently incompatible with most organic polymers, several methods have been studied to make clay compatible with polymers. The most popular involves surface ion exchange, in which the metal cations on the clay's surface are exchanged for organic cationic surfactants, typically ammonium or phosphonium compounds with long alkyl chains.[6,7]

Poly(methyl methacrylate) (PMMA) is a transparent, hard, and stiff material with excellent ultraviolet stability, low water absorption, and outstanding outdoor weathering properties.[8] PMMA/clay nanocomposites are of interest for improved thermal and mechanical properties, reduced flammability, reduced gas permeability, as well as their good potential to retain excellent optical clarity. Different preparation methods for PMMA−clay nanocomposites have been studied, including solution,[9,10] or melt intercalation/exfoliation,[11−19] and in situ polymerization.[20−28] Among them, dispersing in situ polymerization may be the most desirable method for preparing nanocomposites, because the types of nanoparticles and the nature of polymer precursors can vary in a wide range to meet the requirements. In this technique, the modified layered silicate is swollen by a liquid monomer or a monomer solution. The monomer migrates into the galleries of the layered silicate, so that the polymerization reaction can occur between the intercalated sheets. The reaction can be initiated either by heat or radiation, by the diffusion of a suitable initiator, or by an organic initiator or catalyst fixed through cationic exchange inside the interlayer before the swelling step by the monomer. Polymerization produces long-chain polymers within the clay galleries. Under conditions in which intra- and extragallery polymerization rates are properly balanced, the clay layers are delaminated and highly exfoliated nanocomposites are formed.[2]

The literature on the in situ polymerization technique is briefly discussed next. In 2003, Li et al.[22] synthesized PMMA/MMT nanocomposites via in situ intercalative polymerization. The nanocomposites possessed partially exfoliated and partially intercalated structures, while their thermal stability, glass transition temperature (T_g), and mechanical properties were notably improved in comparison with pure PMMA. Moreover, the T_g and the thermal decomposition temperature of the nanocomposites prepared by Xie et al.[23] were 6−15 °C and 100−120 °C higher than those of pure PMMA. Su et al.[24,25] studied the effect of the clay organic modifier on the nanocomposites properties. Either exfoliated or intercalated systems were obtained. Improved thermal stability was revealed from TGA, while the evaluation of mechanical properties showed an increase in Young's modulus along with a decrease in elongation, and an increased tensile strength. Ingram et al.[26] concluded that polymerization was accelerated in the presence of organoclay and that T_g was increased by 20 °C with only a few weight percent of clay. Qu et al.[27] also reported a substantial enhancement of the thermal stability and the mechanical properties of the nanocomposites that they produced. Tsai et al.[28] prepared both exfoliated and intercalated nanocomposites with excellent gas barrier properties. Finally, Dhibar et al.[29] investigated the

* To whom correspondence should be addressed. Tel.: +30 2310 997822. Fax: +30 2310 997769. E-mail: axilias@chem.auth.gr.

10.1021/ie100186a
Published on Web 05/18/2010

Table 1. Chemical Structure of the Organic Modifiers of Different Cloisites Used, Together with Their Cation Exchange Capacity and the d_{001} Spacing Measured from WAXD[a]

Sample	Organic modifier	CEC (meq/100g clay)	d_{001} (Å)
Cloisite Na^+	none	92	11.8
Cloisite 30B	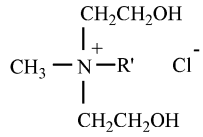	90	17.9
Cloisite 25A	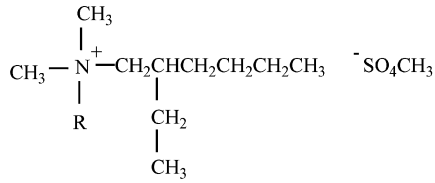	95	19.1
Cloisite 15A	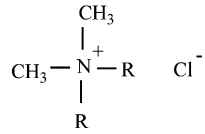	125	29.4

[a] R and R′ are hydrogenated tallow and tallow (~65% C18, ~30% C16, ~5% C14), respectively.

effect of the manufacturing technique on the thermal and mechanical properties of PMMA/clay nanocomposites. A maximum T_g increment and better thermal stability was achieved by the in situ polymerization method.

In this research, an effort was undertaken to synthesize PMMA/MMT nanocomposites by in situ bulk polymerization using different grades of commercial organically modified clay. The effect of the amount of nanofiller and type of organic modifier was investigated. Reaction kinetics was recorded my measuring the variation of conversion with time. The structural and morphological characteristics of the nanocomposites produced were verified with wide angle X-ray diffraction (WAXD), scanning electron microscopy (SEM), and transmission electron microscopy (TEM) analysis, their glass transition temperature was measured with differential scanning calorimetry (DSC), their molecular weight distribution was measured with gel permeation chromatography (GPC), the thermal stability was measured with thermogravimetric analysis (TGA), and the mechanical behavior (tensile properties) with an Instron dynamometer.

Experimental Section

Materials. The methyl methacrylate (MMA) monomer with a purity ≥99% was purchased from Fluka, and the hydroquinone inhibitor was removed by passing it, at least twice, through a disposable inhibitor−remover packed column, supplied from Aldrich, before any use. The free radical initiator, benzoyl peroxide (BPO) with a purity >97%, was provided by Fluka AG and purified by fractional recrystallization twice from methanol, which was purchased from Merck. All other chemicals used were of reagent grade.

For the preparation of the nanocomposites, commercial organically modified montmorillonite clays (OMMTs), Cloisite 15A, Cloisite 25A, and Cloisite 30B, kindly provided by Southern Clay Products Inc. (Texas, USA) were used. These are MMT modified with a quaternary ammonium salt, which is dimethyl hydrogenated tallow, dimethyl 2-ethyl hexyl hydrogenated tallow, and methyl tallow bis-2-hydroxyethyl for Cloisites 15A, 25A, and 30B, respectively. The chemical structures of the ammonium salts and their cationic exchange capacity (CEC) are illustrated in Table 1. Typical physical properties according to the manufacturer were the following: size as measured by a transmission electron microscope for a PA6 nanocomposite 75−150 nm × 1 nm and surface area 750 m^2/g when exfoliated. In addition, sodium containing natural MMT was used under the trade name Cloisite Na^+ and CEC = 92 mequiv/100 g MMT.[30,31]

Preparation of the Initial Monomer−Nanoclay Mixtures. The initial mixture was prepared by dispersing the appropriate amount of OMMT in 25 g of the monomer MMA in a 100 mL conical flask, by adequate magnetic and supersonic agitation. The duration of agitation was varied with the type of MMT used. Thus, the magnetic agitation for the Cloisite Na^+, Cloisite 15A, Cloisite 25A, and Cloisite 30B lasted for 24, 2, 15, and 22.5 h, respectively, while the supersonic agitation was 1 h for all samples. The dispersion of the particles in the monomer was homogeneous, as indicated by the high translucency in the visible region. In the final suspension, BPO 0.03 M was added and the mixture was degassed by passing nitrogen and immediately used.

Synthesis of PMMA/Clay Nanocomposites. Two series of neat PMMA, PMMA/clay nanocomposites containing 1 wt % Cloisite Na^+, 1 wt % Cloisite 30B, 1 wt % Cloisite 25A, and 1 wt % Cloisite 15A and PMMA/clay nanocomposites containing 0.5, 2, 3, and 5 wt % Cloisite 15A were prepared by in situ free radical bulk polymerization.

In the first series, in order to study the reaction kinetics, free radical bulk polymerization was carried out in small test tubes by heating the initial monomer−nanoclay−initiator mixture at 80 °C for a suitable time. According to this technique, 2 mL of

the preweighted mixtures of monomer with the initiator and each Cloisite were placed into a series of 10 test tubes. After degassing with nitrogen, they were sealed and placed into a preheated bath at 80 °C. Each test tube was removed from the bath at 6 min time intervals and was immediately frozen, after the addition of few drops of hydroquinone, in order to stop the reaction. The product was isolated after dissolution in CH_2Cl_2 and reprecipitation in MeOH. The polymers were dried to constant weight in a vacuum oven at room temperature. All final samples were weighed and the degree of conversion was estimated gravimetrically.

In the second series of experiments, specimen were produced for mechanical and thermal property measurements. Since following the above procedure resulted in the formation of undesirable bubbles in the samples due to volume shrinkage or possible monomer evaporation, a slightly different technique was used. Accordingly, free radical bulk polymerization was carried out by heating each mixture, first at 80 °C for a suitable time period, to get a critical viscosity level. Then, the viscous liquid obtained was poured into a mold to finish the polymerization process successfully at 40 °C for 20 h. In each case, standard dumbbells were prepared by following the aforementioned procedure.

Measurements. Wide Angle X-ray Diffraction (WAXD). X-ray diffraction (XRD) patterns were obtained using an X-ray diffractometer (3003 TT, Rich. Seifert) equipped with Cu Kα generator ($\lambda = 0.1540$ nm). Scans were taken in the range of diffraction angle $2\theta = 1-10°$.

Scanning Electron Microscopy (SEM). SEM was carried out using a JEOL JMS-840A scanning microscope equipped with an energy-dispersive X-ray (EDX) Oxford ISIS 300 microanalytical system. For this purpose, fractured surfaces in liquid nitrogen were used. All the studied surfaces were coated with carbon black to avoid charging under the electron beam.

Transmission Electron Microscopy. TEM experiments were carried out on a JEOL 2011 TEM with a LaB6 filament and an accelerating voltage of 200 kV. Samples were prepared by evaporating drops of a PMMA/OMMT nanocomposite−ethanol suspension after sonication onto a carbon-coated lacy film supported on a 3 mm diameter, 300 mesh copper grid.

Gel Permeation Chromatography (GPC). The molecular weight distribution and the average molecular weights of pristine PMMA and all nanocomposites were determined by GPC. The instrument used was from Polymer Laboratories, model PL-GPC 50 Plus, and included an isocratic pump, a differential refractive index detector, and three PLgel 5 μ MIXED-C columns in series. All samples were dissolved in THF at a constant concentration of 1 mg mL^{-1}. After filtration, 200 μL of each sample was injected into the chromatograph. The elution solvent was THF at a constant flow rate of 1 mL min^{-1}, and the entire system was at a constant temperature of 30 °C. Calibration of GPC was carried out with standard poly(methyl methacrylate) samples (Polymer Laboratories) with peak molecular weight ranging from 690 to 1 944 000.

Mechanical Properties. Tensile tests were conducted on an Instron-BlueHill 2 dynamometer at room temperature, according to the ASTM D638 method. Prior to measurements, the samples were conditioned at 50 ± 5% relative humidity for 36 h and placed in a closed chamber containing a saturated $Ca(NO_3)_2 \cdot 4H_2O$ solution in distilled water (ASTM E-104). The crosshead speed was set at 5 mm min^{-1}, and the initial gauge length was fixed at 22 mm. Five measurements were conducted for each sample, and the results were averaged to obtain a mean value.

Differential Scanning Calorimetry (DSC). In order to estimate the glass transition temperature of every nanocomposite prepared, DSC was used. Samples were initially heated to 180 °C at a rate of 10 °C min^{-1} to ensure complete polymerization of trace amounts of residual monomer. Following this, the samples were cooled to 20 °C and their glass transition temperature was measured by heating again to 180 °C at a rate of 20 °C min^{-1}.

Thermogravimetric Analysis (TGA). The thermal stability of the samples was measured by thermogravimetric analysis. TGA was performed on a Pyris 1 TGA (Perkin-Elmer) thermal analyzer. Samples of about 5−8 mg were used. They were heated from ambient temperature to 600 °C at a heating rate of 10 °C min^{-1} under nitrogen flow.

Results

Structure and Morphology. The distribution of the MMT nanoparticles in the samples was studied with scanning electron microscopy. Figure 1 shows SEM photographs of the nanocomposites. It is obvious that a very satisfactory dispersion of the filler was achieved and only at the highest amount of Cloisite 15A (i.e., that of 5 wt %) were some particulates observed.

Polymer−clay nanocomposites could be characterized as immiscible (tactoids), intercalated, partially exfoliated, or exfoliated. The particular form depends on the clay content, the chemical nature of the organic modifier, and the synthetic method. In general, an exfoliated system is more feasible with lower clay content (about 1 wt %), while an intercalated structure is frequently observed for nanocomposites with higher clay content. XRD results for pure PMMA and the corresponding PMMA nanocomposites with different Cloisites appear in Figure 2a. The *d*-spacings for Cloisite Na^+, Cloisite 25A, and Cloisite 30B were measured as 1.18, 1.91, and 1.79 nm, which are close to the values reported by Southern Clay Products Inc., i.e. 1.17, 1.86, and 1.85 nm, respectively. No significant peak was found for pure PMMA and PMMA nanocomposites, which means that all nanocomposites obtained from the in situ bulk polymerization are exfoliated. Similar behavior has been reported in the literature for nanocomposites of PMMA with Cloisite 93A,[32] Cloisite 30B,[26] and Cloisite Na^+.[27] Moreover, XRD results of Cloisite 15A, pure PMMA, and PMMA nanocomposites with 0.5, 1, 2, 3, and 5 wt % Cloisite 15A appear in Figure 2b. The *d*-spacing for Cloisite 15A was measured as 2.94 nm, close to the 3.15 nm value reported by Southern Clay Products Inc. and larger than that of Cloisite Na^+, indicating that the intercalant certainly intercalates into the silicate layer of MMT. No significant peak was observed for the nanocomposites with 0.5 wt % Cloisite 15A, while a small peak around 2.4° (corresponding to $d = 3.7$ nm) was observed in the nanocomposite containing 1 wt % Cloisite 15A. As the amount of the MMT increases from 2 to 5 wt %, the strong (001) plane peak corresponding to d_{001} (3.7 nm) is clearly observed with increased peak intensity. The d_{001}-spacings of the nanocomposites were 3.7, 3.5, 3.3, and 3.7 nm for compositions 1, 2, 3, and 5 wt %, respectively. No significant trend of the change in *d*-spacing was observed as a function of loading in accordance to other literature findings.[14] Thus, from the XRD patterns, it is suggested that the nanocomposites with higher than 1 wt % Cloisite 15A could be considered as partially exfoliated and intercalated.

TEM observations were used to augment WAXD analysis of the nanostructures. Figure 3 shows indicative TEM micrographs of the PMMA/OMMT nanocomposites where the brighter region represents the polymer matrix while the dark narrow stripes represent the MMT nanoparticles. Notice that in

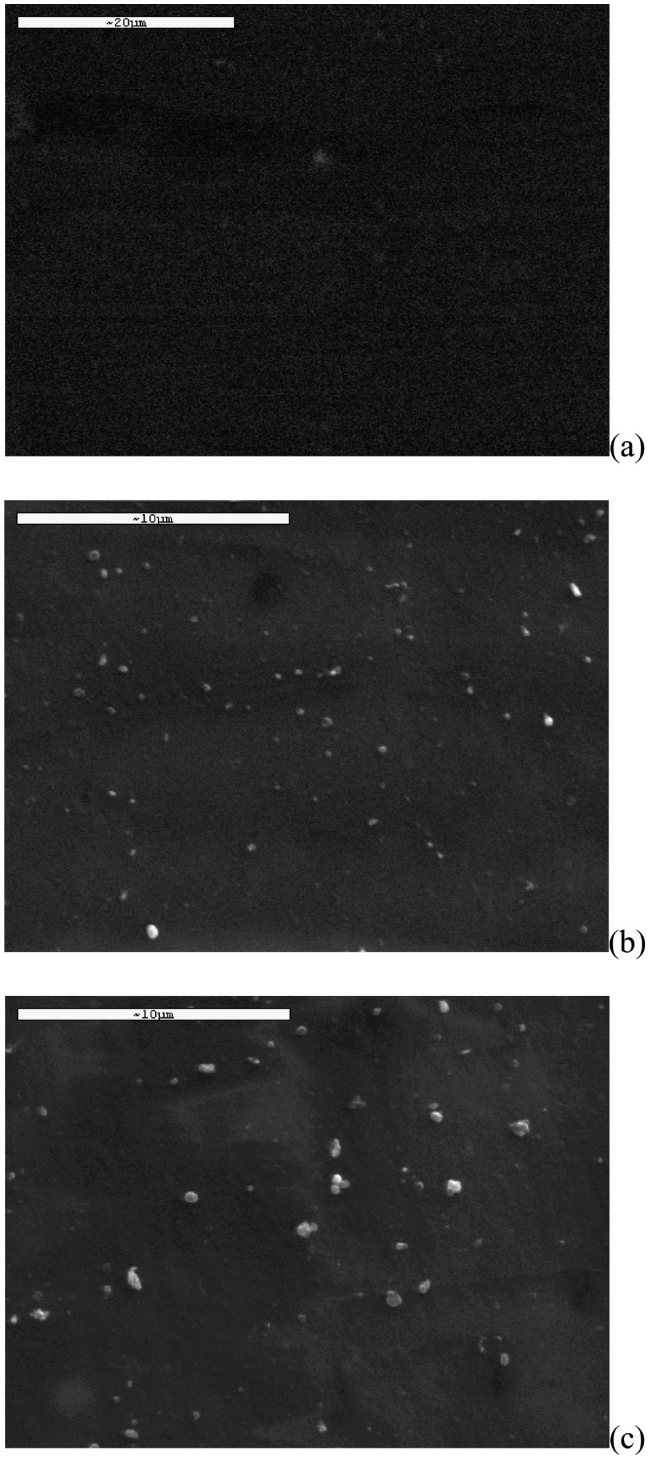

Figure 1. SEM microphotographs of pure PMMA (a) and nanocomposites of PMMA with 2 wt % (b) and 5 wt % (c) Cloisite 15A, showing the dispersion of the nanoparticles (white dots).

order to distinguish between intercalated or exfoliated structures a high magnification has been employed. Figure 3a and b, for nanocomposites with 1 wt % Cloisite 30B or 25A, reveals that individual layers of the MMT are well-dispersed in the PMMA matrix and separated one from the other. This means that OMMT was exfoliated into secondary particles with a thickness lower than 20 nm. With the increase of the OMMT content as shown in Figure 3c and d with 3 and 5 wt % Cloisite 15A, respectively, it was found that MMT layers were also uniformly dispersed in the PMMA matrix. Furthermore, the nanocomposites appear to contain oriented collections of 4−5 parallel silicate

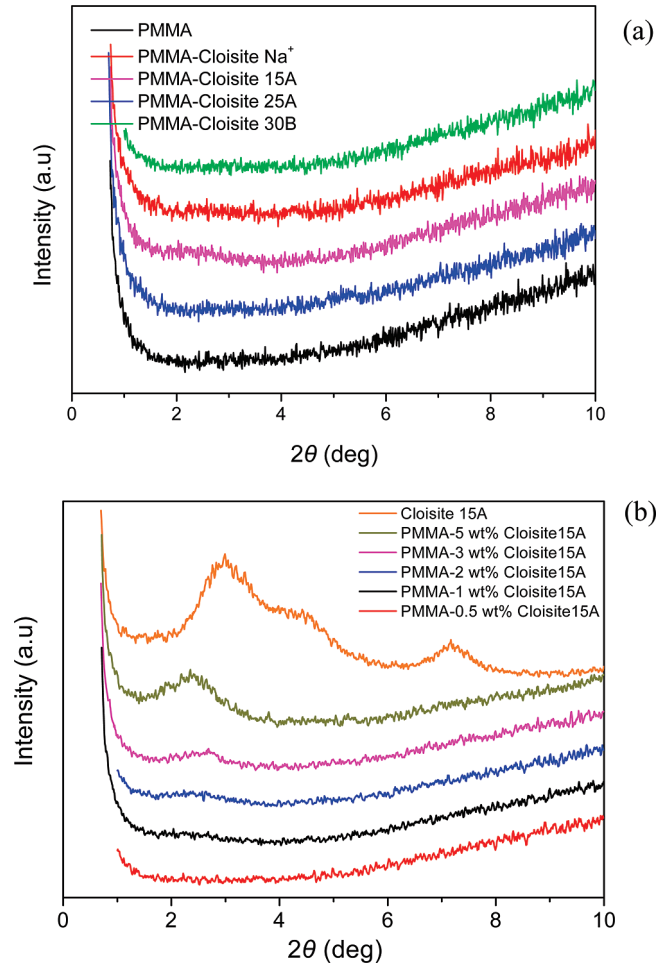

Figure 2. Comparative XRD spectra of PMMA and PMMA nanocomposites with 1 wt % Cloisite Na^+, Cloisite 15A, Cloisite 25A, and Cloisite 30B (a) as well as of Cloisite 15A, PMMA, and PMMA nanocomposites with different amounts of Cloisite 15A (b) obtained from the bulk polymerization of MMA with different OMMT nanoparticles at a constant temperature of 80 °C and initial initiator concentration 0.03 M BPO.

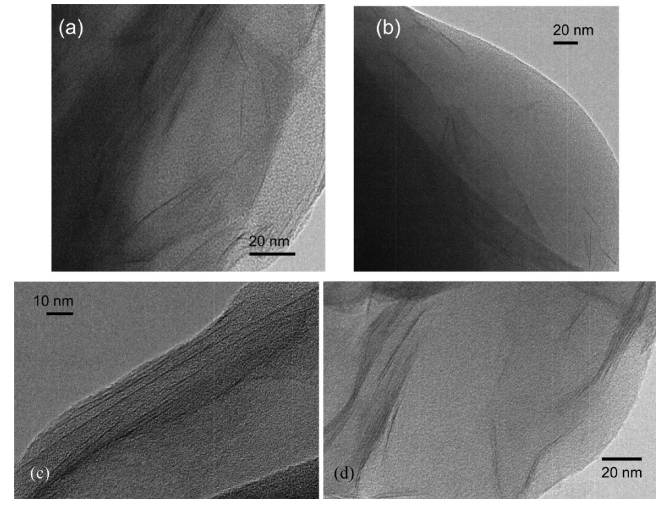

Figure 3. TEM micrographs of PMMA/OMMT nanocomposites containing 1 wt % Cloisite 30B (a), 1 wt % Cloisite 25A (b), 3 wt % Cloisite 15A (c), and 5 wt % Cloisite 15A (d).

layers denoting an intercalated structure in accordance with the WAXD measurements.

Polymerization Kinetics. Results on conversion versus time for pure PMMA and the nanocomposites with 1 wt % of

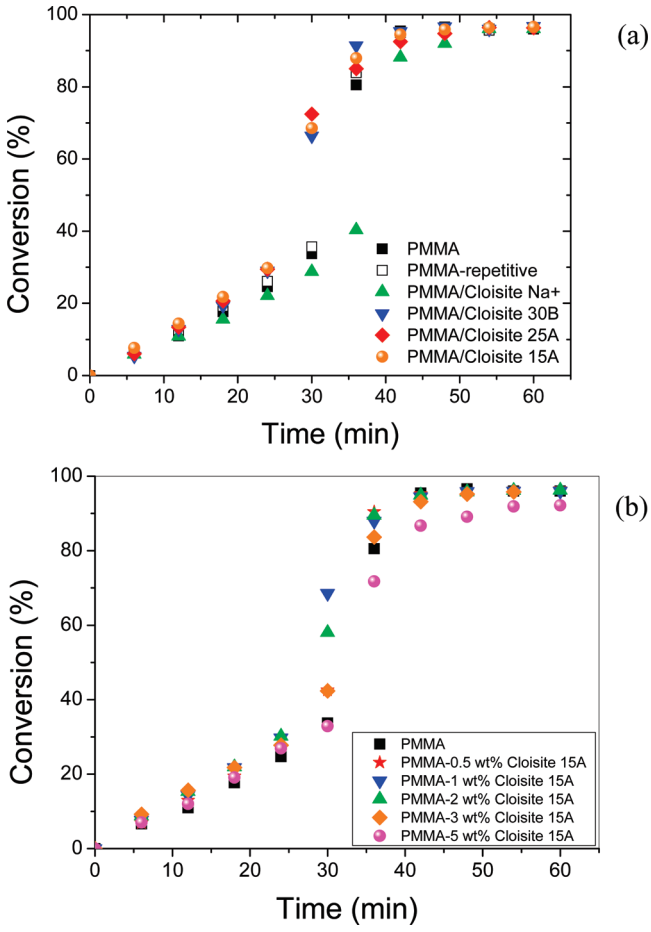

Figure 4. Effect of the type (a) and the amount (b) of nano-MMT on the conversion versus time during bulk polymerization of MMA with 0.03 M BPO at 80 °C.

different Cloisites appear in Figure 4a. In order to test the precision of the data, one repetitive experiment with pure PMMA was carried out and the results are also included in this figure. Very good reproducibility was observed in all conversion ranges (within ±1%). From an inspection of the curves, the typical behavior as in pure PMMA was observed in all experiments. The key points are briefly discussed next.

At low conversion values, the X vs t curves, follow almost "classical" free-radical polymerization kinetics. After a certain point in the region of 20−30% conversion, an abrupt increase in the reaction rate takes place accompanied by an increase in the conversion values. This is the well-known autoacceleration or gel-effect and is attributed to the effect of diffusion-controlled phenomena on the termination reaction and the reduced mobility of "live" macroradicals in order to find one another and react.[33−36] Therefore, their concentration locally increases, leading to increased reaction rates. At approximately 70−80% monomer conversion, the polymerization rate starts falling, and as the reaction proceeds, it tends asymptotically to zero. Consequently, polymerization almost stops before the full consumption of the monomer. Actually, an ultimate conversion around 95−96% was measured. This is a situation that happens when the polymerization temperature is below the glass transition temperature, and at this point, the T_g of the monomer−polymer mixture approaches the reaction temperature; thus, a glassy state appears, and it corresponds to the well-known glass-effect. This is attributed to the effect of diffusion-controlled phenomena on the propagation reaction and the reduced mobility of monomer molecules to find a macroradical and react.[33] From the results

Scheme 1. Entrapment of Free Radicals in an Environment of Exfoliated Organomodified MMT and Polymer Chains, during Bulk Polymerization at High Conversions

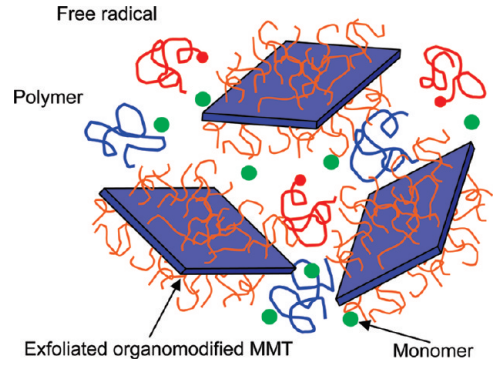

appearing in Figure 4, it seems that the gel-effect starts earlier in the nanocomposites with the OMMT, while it does not seem to depend much on the type of modification. Moreover, the nanocomposites with the unmodified MMT seem to retard the whole conversion vs time curve. One possible explanation could be provided, if we consider the exfoliated OMMT in an environment of reacting macroradicals and polymer macromolecules as in Scheme 1. Then, if a live radical, such as that in the center of the scheme, has to move in space in order to find another and react (translational diffusion), it has to overcome a resistance in its movement not only from its own radicals and polymers but also from the MMT platelets and its organic modifiers (ammonium salts) which constitute large molecules as can be seen in Table 1. Therefore, in an environment with decreasing free volume, the OMMT platelets with the large chemical structure of the modifiers add an extra hindrance in the movement of the macroradicals in space, resulting in locally increased radical concentrations. This is exactly the cause of the gel-effect. Thus, it appears that the presence of OMMT nanoparticles enhances the rate of polymerization and slightly shortens the polymerization time to achieve a specific monomer conversion. In contrast, the unmodified MMT (Cloisite Na^+) seems to act most likely as a radical scavenger, reducing the concentration of live radicals and reducing the reaction rate, or conversion, at a specific time.

By increasing the amount of nanofiller above 1 wt %, it was observed that the conversion values at specified times decreased. Using of 5 wt % Cloisite 15A, the final conversion values were much lower compared to neat PMMA (Figure 4b). It seems that at such high clay loadings and at high conversions, even the diffusion of the small monomer molecules is restricted and therefore their ability to find a radical and react is diminished, resulting in lower monomer conversion values.

Finally, the glass transition temperature of the last sample of neat PMMA and all the nanocomposites was measured, according to the procedure described in the experimental section. Measurements for pure PMMA were around 101−103 °C as is common in PMMA, while the corresponding values for the nanocomposites were found to be around 118 °C, much higher than that of PMMA. More specifically, the values measured for neat PMMA, repetitive neat PMMA, PMMA/Cloisite Na^+, PMMA/Cloisite 15A, PMMA/Cloisite 25A, and PMMA/Cloisite 30B were 101, 103, 117.8, 118.2, 117.7, and 116.4 °C, respectively. Change in the T_g of the polymer matrix with the addition of nanosized particles is another "nanoeffect" noted in the literature, with both increases and decreases reported, dependent upon the interaction between the matrix and the particle.[4] In order to provide an explanation for this observation,

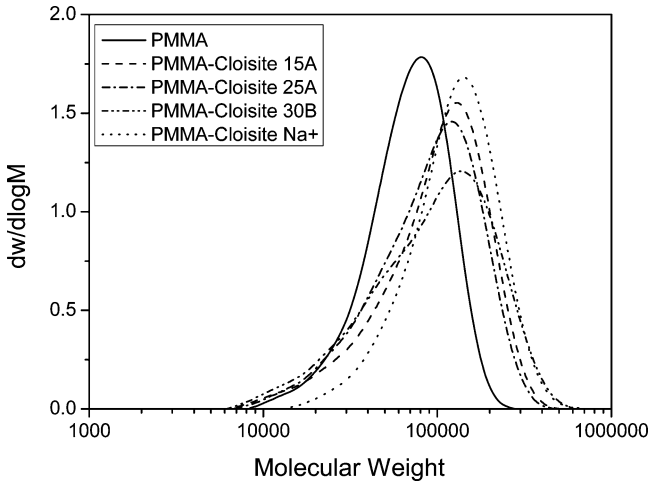

Figure 5. Molecular weight distribution of neat PMMA and PMMA nanocomposites.

the full molecular weight distribution (MWD) of all samples was measured. Results for neat PMMA and PMMA/nanocomposites appear in Figure 5. As it can be seen, the full MWD of all nanocomposites is shifted to higher values. The number average molecular weight of neat PMMA, PMMA/Cloisite Na^+, PMMA/Cloisite 15A, PMMA/Cloisite 25A, and PMMA/Cloisite 30B was 62 360, 112 950, 78 820, 75 320, and 74 290, respectively. Therefore, the increase in T_g with the addition of the nanofiller could be attributed to the production of materials with higher average molecular weight compared to neat PMMA. This in turn can be explained by the increase in the length of the macroradicals before they find one another and terminate, due to the hindrance in their movement in space caused by the presence of the nanofiller as was reported earlier.

Thermal Properties. Figures 6 and 7 show curves for TGA measurements used to determine the mass loss (a) or differential mass loss (b) due to thermal degradation of the nanocomposites. More specifically, the effect of the amount of Cloisite 15A is presented in Figure 6a and b, while the effect of the type of MMT is in Figure 7a and b. From both figures, it is clear that the thermal stability of the PMMA/MMT nanocomposites noticeably improved compared to pure PMMA, as it is expressed by a shifting of the degradation curve to higher temperatures. The origin of this noticeable increase in the decomposition temperatures has been attributed to the ability of nanometer silicate layers to obstruct volatile gas produced by thermal decomposition. Accordingly, thermal decomposition begins from the surface of the nanocomposites, leading in an increase of the organo-MMT content and the formation of a "protection layer" by the clay. This so-called "barrier model" may work well for char-forming polymers, but it seems to not hold for nonchar-forming polymers such as PMMA or PS.[37,38] According to Vyazovkin et al.,[37,38] nanoconfinement appears to present a more specific description of the phenomenon. According to this theory, polymer degradation starts and the newly formed radicals are nanoconfined, permitting a variety of bimolecular reactions to occur. As degradation progresses, the clay platelets, driven by a decrease in the surface free energy, migrate gradually to the surface and form the barrier that has been also detected experimentally.

From the results included in Figure 6, it is clear that the $T_{10\%}$ (i.e., temperature at 10% degradation) increases as much as 40 °C with the addition of 3 wt % Cloisite 15A, while a further increase of the amount of MMT to 5 wt % does not improve significantly the thermal stability of the nanocomposite. A

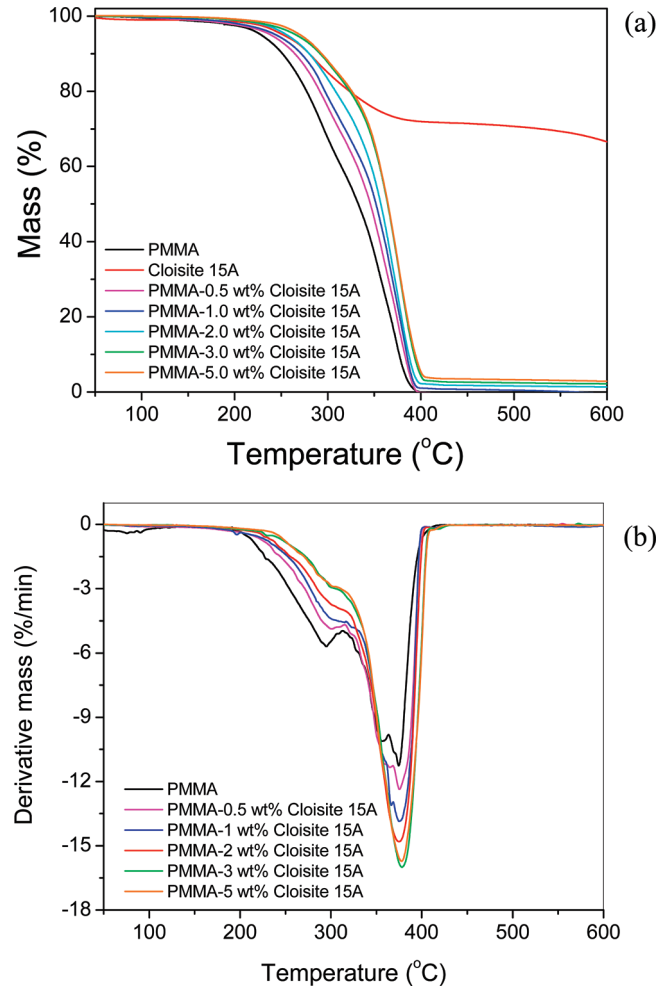

Figure 6. TGA (a) and DTGA (b) scans of PMMA/Cloisite 15A nanocomposites at various clay weight fractions. The heating rate is 10 °C/min.

leveling off of the nanocomposites' thermal stability with clay loading greater than 6 wt % has been also reported in the literature.[14] From the DTGA curves, a triple peak was observed in the case of PMMA, meaning a degradation mechanism taking place in three separate steps. These have been attributed to the degradation of weak links in the polymer chain, degradation arising from end chain unsaturation, and the third and largest step is ascribed to random scission.[39] It is clear that as the amount of Cloisite increases the initial step (first peak at the lowest temperature) is significantly decreased, while the third step (at the highest temperature) is increased. This means a protection of the degradation at low temperatures which has been probably attributed to the templating effect.[21]

Concerning the type of Cloisite used, it is seen that the addition of the nature MMT (Cloisite Na^+) does not offer any improvement in the thermal stability of the nanocomposites with all characteristic temperatures approximately equal to the corresponding value of neat PMMA. This is in contrast to the findings of Kumar et al.,[19] where a significant improvement in the thermal stability was observed. The reason may be the much larger amount of nanofiller used by these authors (i.e., 10 wt %), compared to the only 1 wt % used in this study. The addition of Cloisite 15A or Cloisite 30B results in approximately the same thermal degradation curve with a significant improvement in the ability of the hybrid to withstand degradation and an increase in the $T_{10\%}$ by 20 and 15 °C, respectively. The best thermal stability with an increase in $T_{10\%}$ by almost 28 °C was

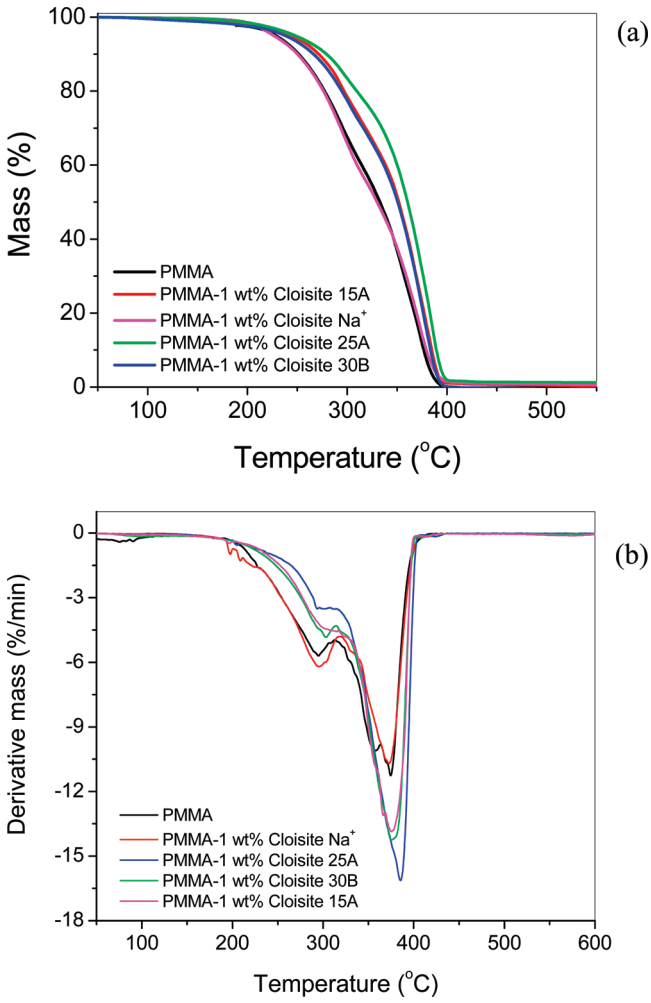

Figure 7. TGA (a) and DTGA (b) scans of PMMA and PMMA nanocomposites with various OMMTs. The amount of clay is 1 wt %, and the heating rate is 10 °C/min.

observed in the nanocomposites formed when Cloisite 25A was used. Also in the DTGA curve, the nanocomposites with Cloisite 25A presented the largest peak at high temperatures and the smallest at low temperatures. One possible explanation for this behavior could be the higher thermal stability of the organic modifier, which in the case of Cloisite 25A is single tallow with an ethylhexyl group compared to Cloisite 30B which included single tallow with two ethanol groups. It should be noticed here that also Cloisite 25A presented the best thermal degradation characteristics, when was used in PMMA based nanocomposites via melt intercalation in the work of Kumar et al.[19] Finally, concerning the final residue, it was noticed that it was zero in the case of pure PMMA and slightly above zero with the 0.5 wt % Cloisite 15A. The percentage of residue at completion of degradation for different amounts of clay was found to increase with clay content in the matrix, as expected in an almost linear way. The residue in the Cloisite Na^+ nanocomposites was exactly the same with the initial amount loaded, since this clay does not have any organic modifier to decompose.

Mechanical Properties. The effect of the different OMMT type and the content of Cloisite 15A on tensile properties such as tensile Young's modulus, tensile strength, and strain at break was investigated, and results are represented in Table 2. For all specimens studied, a typical behavior of a hard and brittle material was observed.

For the study of the different OMMT type effect on the mechanical properties of the nanocomposites, 1 wt % loading was used for all Cloisite samples. It is obvious that nanocomposites containing Cloisite 15A and Cloisite 25A yielded the maximum values of tensile strength and tensile Young's modulus. Particularly, an augmentation of 5.1% and 5.4% in tensile strength was observed for Cloisite 15A and Cloisite 25A, respectively, as well as a tensile modulus increase by about 4.9% for both OMMTs comparing to pristine PMMA. With respect to Cloisite 30B, the tensile strength value was maintained at the same level with pure PMMA, while the tensile modulus increased by about 2.5%. On the contrary, nanocomposites containing Cloisite Na^+ exhibited lower values of tensile strength and modulus. In this case, a decrease of 11.5% was observed for both quantities.

According to the structural characteristics of nanoclays (Table 1), Cloisite 15A and 25A seem to be more hydrophobic systems than Cloisite 30B and Cloisite Na^+, due to their ammonium salt nature, and more compatible with PMMA. It is worthy to point out that ammonium salt of Cloisite 15A and 25A have nonpolar ligands, whereas Cloisite 30B contains ligands with polar OH groups. Consequently, the augmentative tendencies in tensile strength and tensile modulus of the nanocomposites obtained with Cloisite 15A and 25A could be attributed to the better compatibility of these OMMT types with the organic phase, resulting in a more homogeneous dispersion into the polymeric matrix. Moreover, strong chemical interactions could take place between OMMT and PMMA into the formed nanocomposite. In this case, the intercalant quaternary ammonium salts of the OMMTs act as the "bridge" connecting the MMT layers and polymer chains. The cationic head groups of the organic modifier molecules reside at the silicate layer, and the organic tail radiates away from the silicate surface and points to the PMMA molecular chains. In addition, other chemical interactions might also be taken into account, resulting from the in situ intercalative polymerization.[22] However Cloisite Na^+ is a natural MMT, not organomodified and absolutely hydrophilic with poor dispersion into the PMMA matrix. As a result, the tensile strength and modulus of PMMA deteriorated in the presence of Cloisite Na^+ nanoparticles. On the other hand, the strain at break, which is an indicator of impact resistance, was the highest for PMMA/Cloisite 30B nanocomposites, probably due to the formation of hydrogen bonding between

Table 2. Values of Tensile Strength, Strain at Break, and Tensile Young's Modulus for PMMA and All PMMA/MMT Nanocomposites Investigated

sample	tensile strength (MPa)	strain at break (%)	tensile Young's modulus (GPa)
PMMA	38.06 ± 2.05	4.03 ± 0.36	1.22 ± 0.08
PMMA/1 wt % Cloisite Na^+	33.72 ± 2.77	4.07 ± 0.38	1.08 ± 0.05
PMMA/1 wt % Cloisite 30B	38.00 ± 1.81	4.55 ± 0.56	1.25 ± 0.05
PMMA-1 wt % Cloisite 25A	40.10 ± 0.93	3.90 ± 0.40	1.28 ± 0.03
PMMA/1 wt % Cloisite 15A	40.00 ± 0.95	3.70 ± 0.29	1.27 ± 0.04
PMMA/0.5 wt % Cloisite 15A	38.31 ± 1.86	4.37 ± 0.20	1.22 ± 0.06
PMMA/2 wt % Cloisite 15A	32.28 ± 1.19	3.40 ± 0.49	1.28 ± 0.03
PMMA/3 wt % Cloisite 15A	25.38 ± 0.81	2.12 ± 0.18	1.32 ± 0.05
PMMA/5 wt % Cloisite 15A	14.76 ± 1.07	1.15 ± 0.12	1.34 ± 0.04

the hydroxyl groups in Cloisite 30B and carbonyl groups in PMMA, while Cloisite 15A and 25 A imparted inferior values to PMMA. One of the factors which contributes to losses in impact strength is the exfoliation degree of the clay in nanocomposites. The tactoids from some possible unexfoliated platelets of Cloisite 15A and 25A can act as stress concentrators thus contributing to loss in impact.[40]

Furthermore, Cloisite 15A was selected for the investigation of the clay content effect on tensile properties of PMMA nanocomposites, because it demonstrates the highest hydrophobicity. Data in Table 2 reveal that Cloisite 15A loading can improve the tensile modulus gradually, against tensile strength and strain at break that both generally decreased. Liaw et al.[11] concluded a similar effect of Cloisite 15A content on tensile properties, when they prepared PMMA/clay nanocomposites by twin-screw compounding. The same results were also obtained from Tiwari and Natarajan[14] for PMMA/Cloisite 10A nanocomposites prepared by melt intercalation. As mentioned before, 1 wt % clay content led to 4.9% and 5.1% increments in tensile modulus and tensile strength, correspondingly, while the strain at break was reduced by about 8.2%. The aforementioned clay content comprises a crucial point for tensile strength, as the nanocomposite gains the optimum strength. In the work of Tiwari and Natarajan,[14] this maximum was observed at 2 wt % clay loading, while in that of Qu et al.,[27] at 0.6 wt %. In addition, the maximum value in strain at break was obtained for 0.5 wt % Cloisite 15A, while by further clay adding the ultimate strain decreased gradually. It is apparent that, when 5 wt % clay was added, the tensile modulus increased almost 10%, but the tensile strength and the strain at break were reduced by about 61% and 71.5%, respectively. These phenomena showed that, although intercalation of clay with polymer can increase the stiffness of the hybrid system, the interfacial adhesion between the OMMT and the PMMA molecules is not strong enough to sustain large deformations. As a result, the nanocomposites failed early and the tensile strength decreased as well.[10] In addition to this comment, the failure in the mechanical properties with the increasing amount of the OMMT could be attributed to the presence of some particulates (shown in the SEM micrographs, Figure 1) caused by the agglomeration of nanofillers. Large particulates are more apparent for composite with 5 wt % filler loading. These large particulates are detrimental to the mechanical properties of resulting composites.

Conclusions

In this investigation, synthesis and characterization of PMMA/organomodified MMT nanocomposites prepared by in situ bulk polymerization were studied. It was found that the presence of OMMT slightly enhances reaction rate and conversion over the same time period, while sodium MMT acts rather as a reaction retarder. The particular strongest effect of some type of OMMT was attributed to the bulk ammonium salt, used as the organic modifier, and its influence on the effect of diffusion-controlled phenomena taking place during polymerization. The T_g of the nanocomposites was found to be around 118 °C, higher than the corresponding value of neat PMMA (around 102 °C) probably due to their higher average molecular weight. Concerning the tensile properties, it was observed that nanocomposites containing Cloisite 15A and 25A yielded the maximum values of tensile strength and tensile modulus, probably due to the better compatibility of these MMT types with the organic phase, resulting in a more homogeneous dispersion into the polymeric matrix. Moreover, tensile modulus was increased by increasing Cloisite 15A loading, while tensile strength and strain at break decreased. Finally, from the TGA measurements, it was clear that the nanocomposites containing 1 wt % Cloisite 25A exhibited higher thermal stability compared to all other nanocomposites as well as to neat PMMA.

Acknowledgment

We thank very much Southern Clay Products Inc. (Texas, USA) for a generous gift of the Cloisites used in this work, as well as Miss Elpiniki Panayotidou for carrying out the WAXD measurements and Miss Eleni Pavlidou for taking the SEM microphotographs.

Literature Cited

(1) Mai, Y.-W.; Yu, Z.-Z. *Polymer Nanocomposites*; Woodhead Publishing Ltd: Cambridge, 2006.

(2) Pavlidou, S.; Papaspyrides, C. D. A review on polymer-layered silica nanocomposites. *Prog. Polym. Sci.* **2008**, *33*, 1119–1198.

(3) Tjong, S. C. Structural and mechanical properties of polymer nanocomposites. *Mater. Sci. Eng.* **2006**, *R 53*, 73.

(4) Paul, D. R.; Robeson, L. M. Polymer nanotechnology: Nanocomposites. *Polymer* **2008**, *49*, 3187.

(5) Zeng, C.; Lee, L. J. Poly(methyl methacrylate) and polystyrene/clay nanocomposites prepared by in situ polymerization. *Macromolecules* **2001**, *34*, 4098–4103.

(6) Vaia, R.; Teukolsky, R.; Giannelis, E. Interlayer structure and molecular environment of alkylammonium layered silicates. *Chem. Mater.* **1994**, *6*, 1017.

(7) Xie, W.; Gao, Z.; Pan, W.; Hunter, D.; Singh, A.; Vaia, R. Thermal degradation chemistry of alkyl quaternary ammonium montmorillonite. *Chem. Mater.* **2001**, *13*, 2979.

(8) Wang, T.-L.; Hwang, W.-S.; Yeh, M.-H. Preparation, properties and anticorrosion application of poly(methyl methacrylate)/montmorillonite nanocomposites coating on brass via solution polymerization. *J. Appl. Polym. Sci.* **2007**, *104*, 4135–4143.

(9) Gao, Z.; Xie, W.; Hwu, J. M.; Wells, L.; Pan, W. P. The characterization of organic modified montmorillonite and its filled PMMA nanocomposite. *J. Therm. Anal. Cal.* **2001**, *64*, 467.

(10) Yeh, J.; Liou, S.; Lai, M.; Chang, Y.; Huang, C.; Chen, C. P.; Jaw, J. H.; Tsai, T. Y.; Yu, Y. H. Comparative studies of the properties of poly(methyl methacrylate)/clay nanocomposite materials prepared by in situ emulsion polymerization and solution dispersion. *J. Appl. Polym. Sci.* **2004**, *94*, 1936.

(11) Liaw, J.-H.; Hsueh, T.-Y.; Tan, T.-S.; Wang, Y.; Chiao, S.-M. Twin-screw compounding of poly(methyl methacrylate)/montmorillonite nanocomposites: effects of compounding temperature and matrix molecular weight. *Polym. Int.* **2007**, *56*, 1045–1052.

(12) Shen, Z.; Simon, G. P.; Cheng, Y. Nanocomposites of PMMA and organically modified layered silicates by melt intercalation. *J. Appl. Polym. Sci.* **2004**, *92*, 2101.

(13) Zheng, X.; Jiang, D. D.; Wilkie, C. A. Methyl methacrylate oligomerically-modified clay and its poly(methyl methacrylate) nanocomposites. *Thermochim. Acta* **2005**, *435*, 202.

(14) Tiwari, R. R.; Natarajan, U. Thermal and mechanical properties of melt processed intercalated poly(methyl methacrylate)-organoclay nanocomposites over a wide range of filler loadings. *Polym. Int.* **2008**, *57*, 738–743.

(15) Laachachi, A.; Ruch, D.; Addiego, F.; Ferriol, M.; Cochez, M.; Lopez Cuesta, J.-M. Effect of ZnO and organo-modified montmorillonite on thermal degradation of PMMA nanocomposites. *Polym. Degrad. Stab.* **2009**, *94*, 670–678.

(16) Si, M.; Goldman, M.; Rudomen, G.; Gelfer, M.; Sokolov, J. C.; Rafailovich, M. H. Effect of clay type on structure and properties of PMMA/clay nanocomposites. *Macromol. Mater. Eng.* **2006**, *291*, 602–611.

(17) Kim, Y.; White, J. L. Formation of polymer nanocomposites with various organoclays. *J. Appl. Polym. Sci.* **2005**, *96*, 1888–1896.

(18) Matadi, R.; Makradi, A.; Ahzi, S.; Sieffert, J. G.; Etienne, S.; Rush, D.; Vaudemont, R.; Muller, R.; Bouquey, M. Preparation, structural characterization and thermomechanical properties of poly(methyl methacrylate)/organoclay nanocomposites by melt intercalation. *J. Nanosci. Nanotechnol.* **2009**, *9*, 2923–2930.

(19) Kumar, S.; Jog, J. P.; Natarajan, U. Preparation and characterization of poly(methyl methacrylate)-clay nanocomposites via melt intercalation: The effect of organoclay on the structure and thermal properties. *J. Appl. Polym. Sci.* **2003**, *89*, 1186.

(20) Choi, Y. S.; Ham, H. T.; Chung, I. J. Polymer/silicate nanocomposites synthesized with potassium persulfate at room temperature: polymerization mechanism, characterization and mechanical properties of the nanocomposites. *Polymer* **2003**, *44*, 8147.

(21) Jash, P.; Wilkie, C. A. Effects of surfactants on the thermal and fire properties of poly(methyl methacrylate)/clay nanocomposites. *Polym. Degrad. Stab.* **2005**, *88*, 401.

(22) Li, Y.; Zhao, B.; Xie, S.; Zhang, S. Synthesis and properties of poly(methyl methacrylate)/ montmorillonite nanocomposites. *Polym. Int.* **2003**, *52*, 892–898.

(23) Xie, T.; Yang, G.; Fang, X.; Ou, Y. Synthesis and characterization of poly(methyl methacrylate)/montmorillonite nanocomposites by *in situ* bulk polymerization. *J. Appl. Polym. Sci.* **2003**, *89*, 2256–2260.

(24) Su, S.; Wilkie, C. A. Exfoliated poly(methyl methacrylate) and polystyrene nanocomposites occur when the clay cation contains a vinyl monomer. *J. Polym. Sci., Part A: Polym. Chem.* **2003**, *41*, 1124–1135.

(25) Su, S.; Jiang, D. D.; Wilkie, C. A. Methacrylate modofied clays and their polystyrene and poly(methyl methacrylate) nanocomposites. *Polym. Adv. Technol.* **2004**, *15*, 225–231.

(26) Ingram, S.; Dennis, H.; Hunter, I.; Liggat, J.; McAdam, C.; Pethrick, R. A.; Schaschke, C.; Thomson, D. Influence of clay type on exfoliation, cure and physical properties of *in situ* polymerised PMMA nanocomposites. *Polym. Int.* **2008**, *57*, 1118–27.

(27) Qu, X.; Guan, T.; Liu, G.; She, Q.; Zhang, L. Preparation, structural characterization and properties of poly(methyl methacrylate)/montmorillonite nanocomposites by bulk polymerization. *J. Appl. Polym. Sci.* **2005**, *97*, 348–57.

(28) Tsai, T.-Y.; Wen, C.-K.; Chuang, H.-J.; Lin, M.-J.; Ray, U. Effect of clay with different cation exchange capacity on the morphology and properties of poly(methyl methacrylate)/clay nanocomposites. *Polym. Compos.* **2009**, *30*, 1552–1561.

(29) Dhibar, A. K.; Mallick, S.; Rath, T.; Khatua, B. B. Effect of clay platelet dispersion as affected by the manufacturing technique on thermal and mechanical properties of PMMA-clay nanocomposites. *J. Appl. Polym. Sci.* **2009**, *113*, 3012–18.

(30) Fan, X.; Xia, C.; Advincula, R. C. Grafting of polymers from clay nanoparticles via in situ free radical surface-initiated polymerization: Monocationic versus bicationic initiators. *Langmuir* **2003**, *19*, 4381–4389.

(31) Zhao, H.; Argoti, S. D.; Farrell, B. P.; Shipp, D. A. Polymer-silicate nanocomposites produced by in situ atom transfer radical polymerization. *J. Polym. Sci., Part A: Polym. Chem.* **2004**, *42*, 916–924.

(32) Kim, S.; Wilkie, C. A. Transparent and flame retardant PMMA nanocomposites. *Polym. Adv. Technol.* **2008**, *19*, 496–506.

(33) Achilias, D. S. A review of modelling of diffusion controlled polymerization reactions. *Macromol. Theory Simul.* **2007**, *16*, 319.

(34) Achilias, D. S.; Verros, G. D. Modelling of diffusion-controlled reactions in free-radical solution and bulk polymerization. Model validation by DSC experiments. *J. Appl. Polym. Sci.* **2010**, *116*, 1842–1856.

(35) Verros, G. D.; Achilias, D. S. Modelling gel-effect in branched polymer systems: Free-radical solution polymerization of vinyl acetate. *J. Appl. Polym. Sci.* **2009**, *111*, 2171–2185.

(36) Achilias, D. S.; Kiparissides, C. Modelling of diffusion-controlled free-radical polymerization reactions. *J. Appl. Polym. Sci.* **1988**, *35*, 1303–1323.

(37) Chen, K.; Wilkie, C. A.; Vyazovkin, S. Nanoconfinement revealed in degradation and relaxation studies of two structurally different polystyrene-clay systems. *J. Phys. Chem. B* **2007**, *111*, 12685–12692.

(38) Vyazovkin, S.; Dranca, I.; Fan, X.; Advincula, R. Degradation and relaxation kinetics of polystyrene-clay nanocomposites prepared by surface-initiated polymerization. *J. Phys. Chem. B* **2004**, *108*, 11672–11679.

(39) Peterson, J. D.; Vyazovkin, S.; Wight, C. A. Kinetic study of stabilizing effect of oxygen on thermal degradation of poly(methyl methacrylate). *J. Phys. Chem. B* **1999**, *103*, 8087–8092.

(40) Beall, G. W.; Tsipursky, S. J. *Chemistry and Technology of Polymer Additives*; Al-Malaika, S., Golovoy, A., Wilkie, C. A., Eds.; Blackwell Science: London, 1999; Chapter 15.

Received for review January 26, 2010
Revised manuscript received May 4, 2010
Accepted May 5, 2010

IE100186A